Computer simulations of a polyelectrolyte chain with a mixture of multivalent salts

2005 J. Phys.: Condens. Matter 17 5635

(http://iopscience.iop.org/0953-8984/17/37/002)

INSTITUTE OF PHYSICS PUBLISHING JOURNAL OF PHYSICS: CONDENSED MATTER

J. Phys.: Condens. Matter **17** (2005) 5635–5645 doi:10.1088/0953-8984/17/37/002

Computer simulations of a polyelectrolyte chain with a mixture of multivalent salts

J Kłos[1] **and T Pakula**[2]

[1] Faculty of Physics, A Mickiewicz University, Umultowska 85, 61-614 Poznań, Poland
[2] Max-Planck-Institute for Polymer Research, Postfach 3148, 55021 Mainz, Germany

Received 9 June 2005, in final form 27 July 2005
Published 2 September 2005

Abstract
Diluted solutions of a single, electrically charged polymer chain, its monovalent counterions and two kinds of multivalent salts are investigated. In particular, the influence of the salt concentrations and valences on the mean effective charge per monomer, total inner energy, radius of gyration and various pair correlation functions of the monomers and free ions are analysed. The calculations show that it is the four-valent and three-valent ions, oppositely charged to the monomers, that mostly occupy the space around the polymer and tremendously increase their number there compared to that in the bulk. Furthermore, reductions in the polymer size and effective charge per monomer appear, especially for increasing amount of the four-valent salt. Thus, there is an evidence for polymer conformational changes associated with the ion condensation onto the chain.

1. Introduction

In spite of intensive research that has been carried out for years, polyelectrolytes in dilute solutions are still very challenging and attractive systems to study. This is because they constitute an important class of materials with great potential for technological applications (to name but a few, water absorption, gel stabilization, surface modification, micro-encapsulation) on one hand, and with difficulties in both experimental and theoretical treatment, on the other [1]. Actually, the effective net charge of a chain and condensation of ions onto it are very classical, though not fully clarified, issues; starting with the work of Manning, many papers have been devoted to these issues [2–25]. Other interesting and crucial subjects of the day include concentration, valence and distribution around the chain of the counterions and salt and the role these particles play in causing the polymer to undergo some conformational changes [22, 26–28]. Due to prospective applications in modern medicine and biotechnology, some low temperature effects (such as the so-called charge inversion) in highly charged biological systems are also intensively studied [29, 30]. Furthermore, the question of the effect of salt, and its concentration, appears in the research on the osmotic pressure of

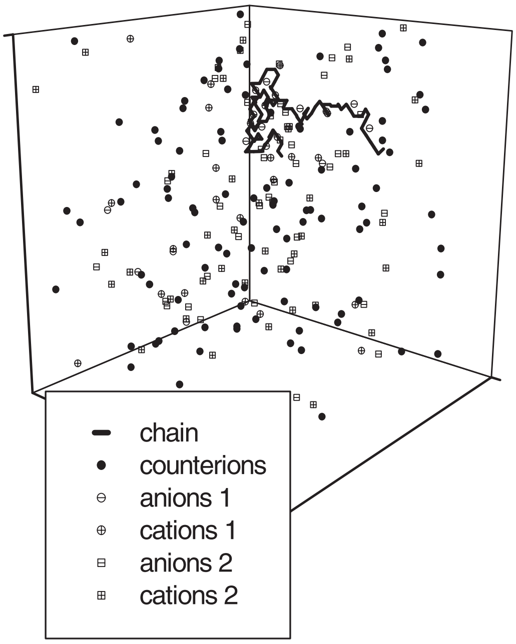

Figure 1. The configuration snapshot recorded for $T^* = 1.0$, $n_{s1} = 20$, $n_{s2} = 40$ $z_{s1} = 4$ and $z_{s2} = 3$.

polyelectrolytes [31–36]. It should also be stressed that at present, for many current questions, computer simulations are the only available source of information on the behaviour of such systems.

In this paper we report on the numerical investigation of a single polyelectrolyte chain with its counterions and two added salts that, in general, differ from each other in concentration and valence. We pay special attention to the issue of the polymer size and free ion distributions around the chain as these two parameters change. By varying both the number and valence of the salt ions of both kinds, we analyse their effect on the conformational properties of the polymer itself and on the distribution of the free particles around it. We record, under such conditions, the size and effective charge of the polymer, and various radial distribution functions of the ions and monomers. These quantities are calculated by employing lattice Monte Carlo simulations in the canonical ensemble with a version of the cooperative motion algorithm as the tossing scheme.

The remainder of the paper is organized as follows. First, we define the model, the simulation method and the measured quantities. Then, the results of our simulations are presented and discussed. Finally, conclusions and remarks are given.

2. Model and numerical procedure

The model system consists of a single linear chain on the face centred cubic lattice with periodic boundary conditions. A chain is made out of N successive beads connected by rigid bonds of length $a = u\sqrt{2}$, where u is the length unit chosen in this paper. In order to model a polyelectrolyte chain, each monomer carries a unit positive electric charge, whereas N free beads (counterions) carry unit charges of the opposite sign. Furthermore, the two kinds of salt ions are modelled by $2n_{s1}$ and $2n_{s2}$ beads, respectively. Half of them, i.e., n_{s1}, n_{s2}, represent cations (anions) with valence $z_{s1}, z_{s2} > 0$ ($z_{s1}, z_{s2} < 0$), so the system is electrically neutral (see figure 1). The solvent is implicitly included in the simulations by means of its

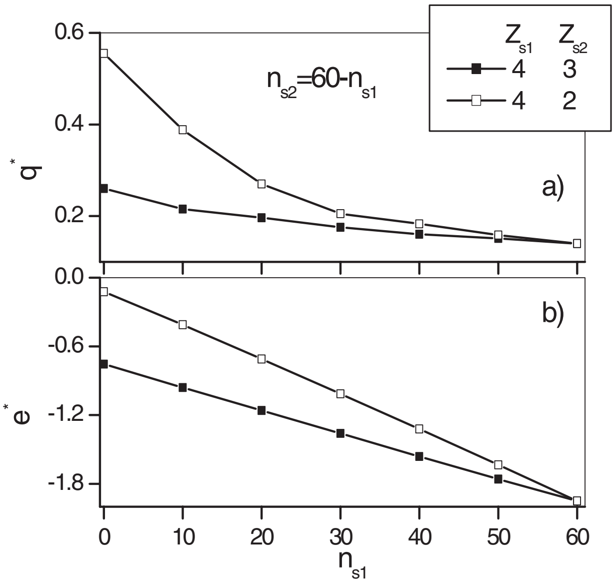

Figure 2. (a) The effective mean charge per monomer q^* versus n_{s1} for $T^* = 1.0$, $z_{s1} = 4$, $z_{s2} = 3, 2$, (b) the average energy per charged element e^* versus n_{s1} for the same parameters as in (a).

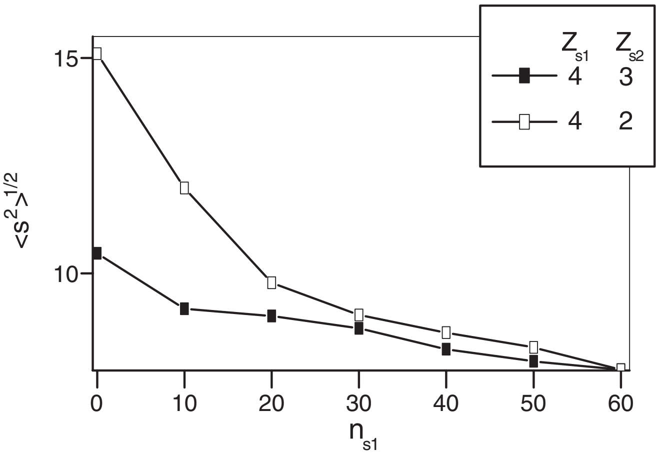

Figure 3. The mean square radius of gyration $\langle s^2\rangle^{1/2}$ versus n_{s1} for the same parameters as in figure 2(a).

permittivity ε. The total Coulomb energy E is given by

$$E = \delta \sum_{i=1}^{n_a-1} z_i \sum_{j>i}^{n_a} z_j \psi_l(r_{ij}), \tag{1a}$$

$$\psi_l(r_{ij}) = \frac{1}{|r_{ij}|} + A_2|r_{ij}|^2 + \sum_{n=4,6}^{l} [A_n O_n(r_{ij}) + B_n P_n(r_{ij})], \tag{1b}$$

where r_{ij} is the nearest-image vector connecting particles i and j, $O_n(r_{ij})$, $P_n(r_{ij})$ are the cubic harmonic solutions to Laplace's equation of the eighth order ($l = 8$), A_n, B_n are the so-

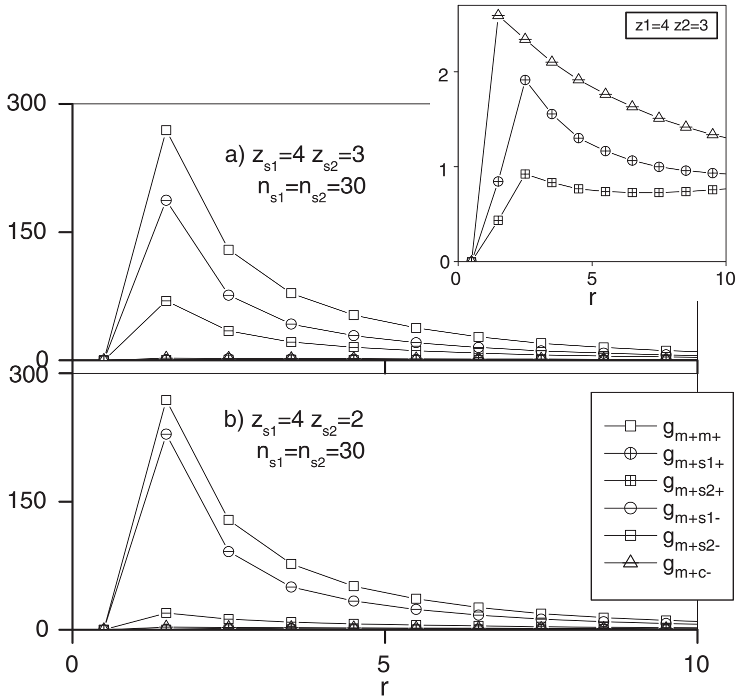

Figure 4. (a) The $g_{m+m+}(r)$, $g_{m+s1+}(r)$, $g_{m+s2+}(r)$, $g_{m+s1-}(r)$, $g_{m+s2-}(r)$, $g_{m+c-}(r)$ PCFs for $T^* = 1.0$, $n_{s1} = n_{s2} = 30$, $z_{s1} = 4$, $z_{s2} = 3$, (b) the same as in (a) except $z_{s2} = 2$.

called optimized coefficients [37], z_i, z_j are the valences of particles i and j, $\delta = e^2/\varepsilon u$ is the energy unit, with e denoting the electric charge, and $n_a = 2(N + n_{s1} + n_{s2})$ is the total number of charges. The pair potential $\psi_l(r_{ij})$ for the cubic periodic boundary conditions provides an accurate approximation of the Ewald summation that should be included in the energy calculations for the Coulomb interactions [37]. In this paper, we calculate thermodynamic averages of various quantities at the reduced temperature T^* defined as $T^* = k_\mathrm{B}T/\delta$, where T is the absolute temperature and k_B is the Boltzmann constant. Furthermore, the excluded volume condition is also taken into account by preventing a lattice site from being occupied by more than one element. Since this is the only short ranged interaction between the monomers, the chain is in a very good athermal solvent. The configurations are tossed by means of a version of the cooperative motion algorithm (CMA; for a detailed description of elementary CMA moves, see [38]) that can be outlined in the following way. (1) A bead (monomer, counterion or salt ion) and one of its neighbouring lattice sites are selected at random. (2) If the latter is empty an elementary CMA move is performed. If the selected bead is a counterion or a salt ion it is moved to the empty site. In this way another empty site (the abandoned one) is generated which is the end of the trial reconfiguration for single, free beads. If the selected bead is a monomer, it is moved to the empty site as well. Furthermore, depending on the local situation encountered, in order that no bonds be broken and that the sequence of beads on the chain and its length be preserved, a number of monomers that follow the selected one are also shifted collectively one after another by subsequently translating by one lattice site until an empty site is finally generated. This is the end of the trial reconfiguration for the monomers. (3) If the lattice site selected in step 1 is occupied, the whole of step 1 is repeated. The new configuration generated in such a way is accepted or rejected according to a probability of the

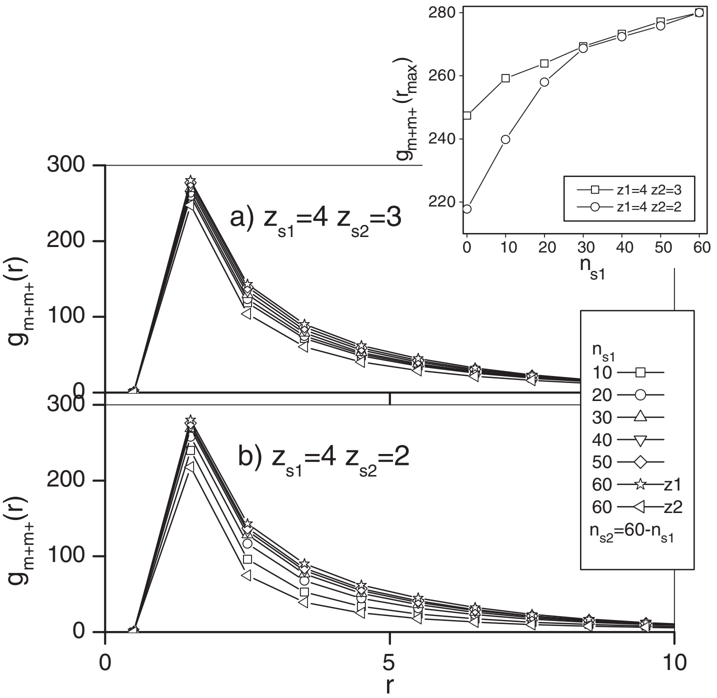

Figure 5. (a) The monomer–monomer PCF $g_{m+m+}(r)$ for $T^* = 1.0$, $n_{s1} = 10, 20, 30, 40, 50, 60$, $z_{s1} = 4$, $z_{s2} = 3$, (b) the same as in (a) except $z_{s2} = 2$. The inset shows the peak heights versus n_{s1} for $z_{s1} = 4$, $z_{s2} = 3, 2$.

Metropolis type [39]:

$$p = \min\left[1, \exp\left(-\frac{\Delta E^*}{T^*}\right)\right], \tag{2}$$

with $\Delta E^* = E^*_{\text{new}} - E^*_{\text{old}}$ (E^*_{new} and E^*_{old} are energies after and before a random reconfiguration, $E^* = E/\delta$).

In the simulations, we have computed the mean square radius of gyration

$$\langle s^2 \rangle = \left\langle \frac{1}{N} \sum_{i=1}^{N} (r_i - r_{\text{cm}})^2 \right\rangle, \tag{3}$$

the mean internal energy per particle $e^* = \langle E^* \rangle (T^*)/n_a$ and the effective mean charge per monomer

$$q^* = 1 + \frac{\sum_t \langle n_t \rangle z_t}{N}, \tag{4}$$

where r_1, r_N denote the position vectors of both ends of the chain, r_i, r_{cm} are the position vectors of the ith monomer and the chain centre of mass, $\langle n_t \rangle$ are the mean numbers of condensed particles of type t with valences z_t (counterions, salt anions and cations; an ion is considered condensed when it occupies a nearest-neighbour site of at least one monomer) and the bracket $\langle\ \rangle$ stands for thermodynamic averaging. Finally, we have also considered various pair correlation functions (PCFs) $g_{ab}(r)$ defined as

$$g_{\alpha\beta}(r) = \frac{\langle N_{\alpha\beta}(r + u) \rangle}{N_\alpha N^{\text{id}}_\beta (r + u)}, \tag{5}$$

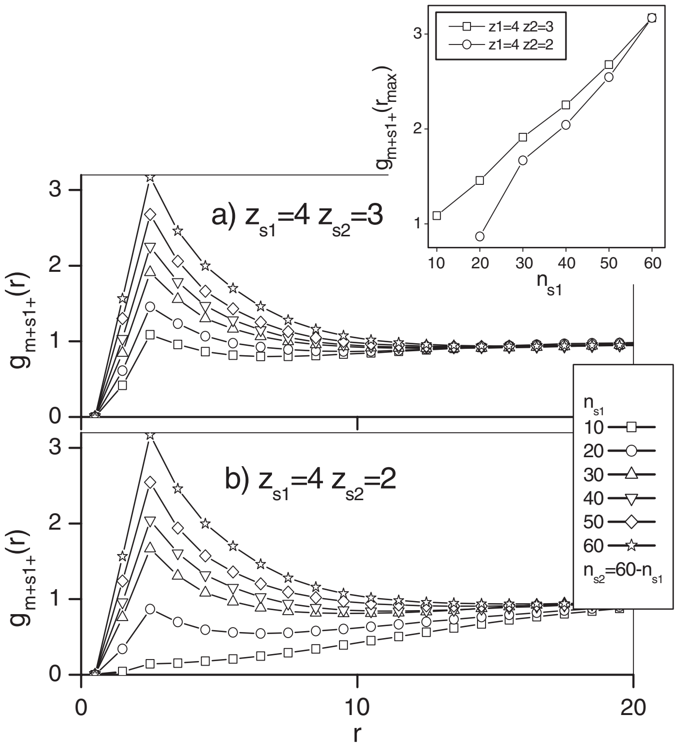

Figure 6. (a) The monomer–positive salt 1 PCF $g_{m+s1+}(r)$ for $T^* = 1.0$, $n_{s1} = 10, 20, 30, 40, 50, 60$, $z_{s1} = 4$, $z_{s2} = 3$, (b) the same as in (a) except $z_{s2} = 2$. The inset shows the peak heights versus n_{s1} for $z_{s1} = 4$, $z_{s2} = 3, 2$.

where the numerator denotes the average number of pairs of particles of type α and β at a relative distance from each other between r and $r + u$, N_α is the total number of particles of type α and $N_\beta^{\mathrm{id}}(r + u)$ is the average number of particles of type β in the ideal gas in the same interval. They include the intramolecular monomer–monomer PCF $g_{m+m+}(r)$, the monomer–salt cation PCF $g_{m+s1+}(r)$, $g_{m+s2+}(r)$, the monomer–salt anion PCF $g_{m+s1-}(r)$, $g_{m+s2-}(r)$ and the monomer–counterion PCF $g_{m+c-}(r)$.

The simulations have been performed on a 3D fcc lattice of size $L^3 = 60 \times 60 \times 60\ \mathrm{u}^3$ for single-chain systems with $N = 100$, $z_{s1} = 4$, $z_{s2} = 3, 2$, $n_{s1} = 0, 10, 20, 30, 40, 50, 60$ and $n_{s2} = 60 - n_{s1}$. Since at room temperature T^* varies between 0.24 and 1, this parameter was set in our simulations to 1 [4]. Typically, at this temperature the number of Monte Carlo steps (one Monte Carlo step is n_a trial reconfigurations) needed for the systems to reach equilibrium was of the order of 10^5.

3. Results

3.1. Effective charge, energy and chain size

In figure 2(a), the mean effective charge per monomer q^* is plotted versus n_{s1} for $z_{s1} = 4$, $z_{s2} = 3, 2$. For the set of parameters taken into account the condensation of ions onto the chain is already well pronounced because q^* is reasonably below one. Furthermore, the observed tendencies are such that $q^*(z_{s1} = 4, z_{s2} = 3) < q^*(z_{s1} = 4, z_{s2} = 2)$ for all

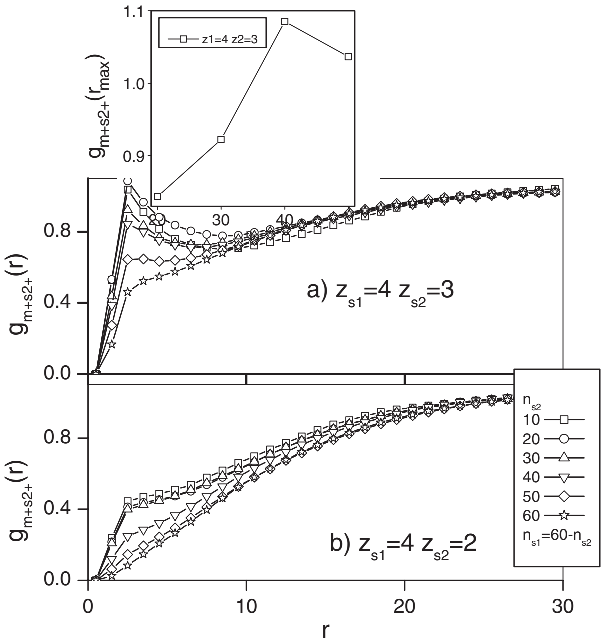

Figure 7. (a) The monomer–positive salt 2 PCF $g_{m+s2+}(r)$ for $T^* = 1.0$, $n_{s1} = 10, 20, 30, 40, 50, 60$, $z_{s1} = 4$, $z_{s2} = 3$, (b) the same as in (a) except $z_{s2} = 2$. The inset shows the peak heights versus n_{s1} for $z_{s1} = 4$, $z_{s2} = 3, 2$.

the values of n_{s1}, n_{s2} considered and that $q^*(n1_{s1}) < q^*(n2_{s1})$ for $n2_{s1} < n1_{s1}$. In other words, the reduction of polymer charge is more pronounced for higher valency of the second salt and increasing number n_{s1} of salt cations (anions) of the first kind (with $z_{s1} = 4$). Furthermore, as indicated by figure 2(b), the behaviour of q^* is well correlated with the average potential energy per charge $e^* = \langle E^* \rangle / n_a$. Actually, the picture again shows that $e^*(z_{s1} = 4, z_{s2} = 3) < e^*(z_{s1} = 4, z_{s2} = 2)$ and that $e^*(n1_{s1}) < e^*(n2_{s1})$ for $n2_{s1} < n1_{s1}$.

Next, we inspect the chain conformations by analysing the average radius of gyration $\langle S^2 \rangle^{1/2}$ versus n_{s1} for $z_{s1} = 4$, $z_{s2} = 3, 2$ that is presented in figure 3. The tendencies with respect to changes in n_s, z_s are again very similar to those previously discussed. Actually, it is clearly seen that $\langle S^2 \rangle^{1/2}(z_{s1} = 4, z_{s2} = 3) < \langle S^2 \rangle^{1/2}(z_{s1} = 4, z_{s2} = 2)$, though the differences become practically indistinguishable for $n_{s1} > 30$. Also, $\langle S^2 \rangle^{1/2}(n1_{s1}) < \langle S^2 \rangle^{1/2}(n2_{s1})$ for $n2_{s1} < n1_{s1}$ which means that the chain reduces its size as the number of the first salt ions increases.

3.2. Pair correlation functions

In the rest of the paper, the local structure of the system is presented via a number of pair correlation functions. A representative example of typical shapes of the PCFs is shown in figure 4 for the system of $n_{s1} = n_{s2} = 30$, $z_{s1} = 4$, $z_{s2} = 3, 2$. Since the values of g_{m+s1+}, g_{m+s2+}, g_{m+c-} are much smaller than g_{m+m+}, g_{m+s1-}, g_{m+s2-}, the former are shown separately in the inset. Generally speaking, the curves possess peaks for a small interparticle distances that indicate the tendency of the particles to increase their number around the polymer in comparison with their number in the bulk. Actually, the high peak of g_{m+m+} is due to the

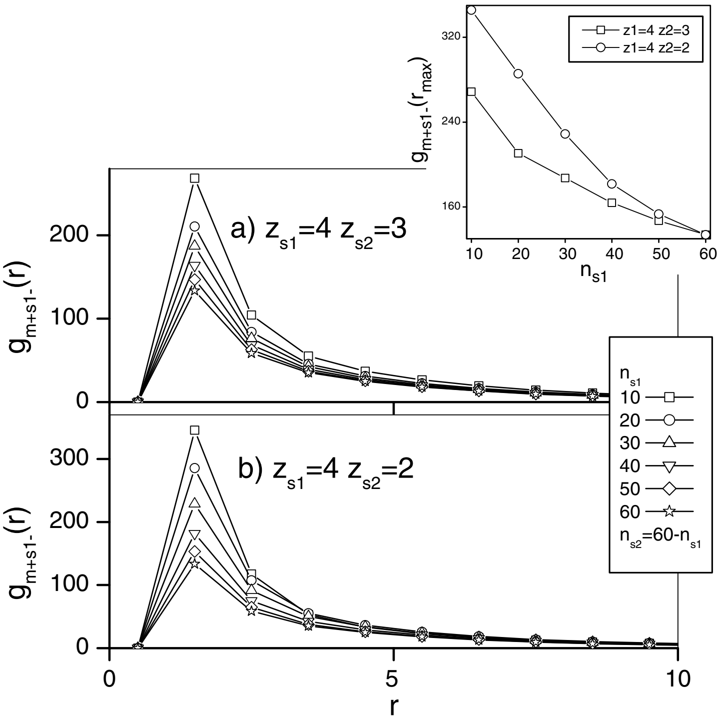

Figure 8. (a) The monomer–negative salt 1 PCF $g_{m+s1-}(r)$ for $T^* = 1.0$, $n_{s1} = 10, 20, 30, 40, 50, 60$, $z_{s1} = 4$, $z_{s2} = 3$, (b) the same as in (a) except $z_{s2} = 2$. The inset shows the peak heights versus n_{s1} for $z_{s1} = 4$, $z_{s2} = 3, 2$.

above-discussed reduction of the polymer size with increasing number n_{s1} of the multivalent salt anions (cations). Our previous studies suggest that the chain is already indeed in a collapsed state [40]. The peaks of g_{m+s1-} and g_{m+s2-}, in turn, demonstrate that the multivalent salt anions strongly concentrate in the vicinity of the chain. Since $g_{m+s1-} > g_{m+s2-}$, this effect is dominated by the four-valent anions. The monovalent counterions and multivalent cations (see the inset) also increase their number near the chain when compared to that for the bulk, though this tendency is much weaker than for the anions. In what follows it is shown in more detail how the PCFs react to changing n_{s1}, n_{s2}.

Figure 5 shows the intramolecular monomer–monomer PCF $g_{m+m+}(r)$ for all the values of n_{s1} and n_{s2} inspected. Each of the curves possesses a clear peak, and in accordance with the previous observations concerning the polymer shape, the inset also shows that the maximum heights increase with increasing amount of the four-valent salt. For $n_{s1} < 30$ the peaks obtained for $z_{s2} = 3$ are higher than those for $z_{s2} = 2$, whereas for $n_{s1} > 30$ they are practically indistinguishable.

Figures 6, 7 show the monomer–salt cation PCF $g_{m+s1+}(r)$, $g_{m+s2+}(r)$ for the same set of parameters as before. The first of them indicates that due to the existence of peaks located relatively close to the monomers, irrespective of the valency of the second salt, the number of the free four-valent cations tends to increase in the vicinity of the polymer when compared to that for the bulk, for increasing n_{s1}. The inset shows that for fixed n_{s1} and n_{s2} the peaks of $g_{m+s1+}(r, z_{s2} = 3)$ are slightly higher than those of $g_{m+s1+}(r, z_{s2} = 2)$. Furthermore, the three-valent cations (see figure 7(a)) also concentrate around the polymer, though in this case

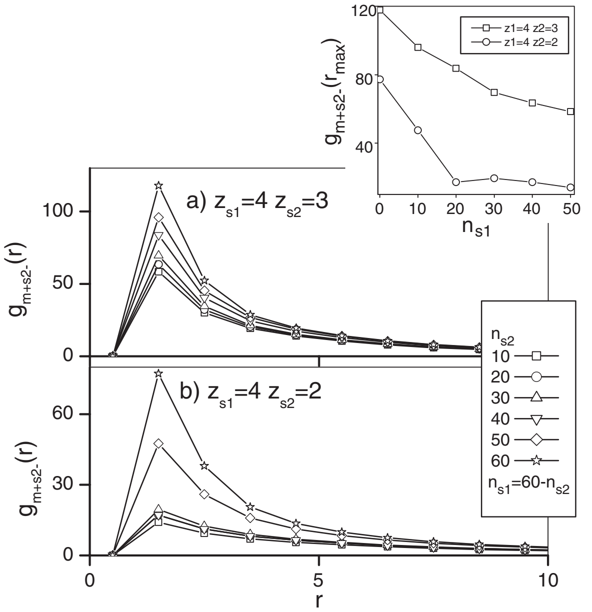

Figure 9. (a) The monomer–negative salt 2 PCF $g_{m+s2-}(r)$ for $T^* = 1.0$, $n_{s1} = 10, 20, 30, 40, 50, 60$, $z_{s1} = 4$, $z_{s2} = 3$, (b) the same as in (a) except $z_{s2} = 2$. The inset shows the peak heights versus n_{s1} for $z_{s1} = 4$, $z_{s2} = 3, 2$.

clear peaks exist only for $n_{s1} > 20$ and are local. The way they change with growing n_{s1} is presented in the inset again. As seen in figure 7(b), we do not observe such grouping of ions near the polyion for $z_{s2} = 2$, and a drop from their number in the bulk in the area of interest occurs, instead.

The distributions of salt anions and counterions around the positively charged monomers $g_{m+s1-}(r)$, $g_{m+s2-}(r)$, $g_{m+c-}(r)$ are presented in figures 8, 9, 10 respectively. In the first two cases there are very high peaks located as close to the monomers as possible for all the values of n_{s1}, n_{s2}, which suggests that a large fraction of these ions are condensed on the chain. This in turn means that the observed reduction of the mean effective charge per monomer q^* is mainly due to them. Furthermore, unlike in the cations case, in this case the peak heights, though large, decrease with increasing number of four-valent salt ions. For fixed n_{s1}, n_{s2}, the maximal value of $g_{m+s1-}(r, z_{s2} = 3)$ is smaller than that of $g_{m+s1-}(r, z_{s2} = 2)$, that is opposed to $g_{m+s2-}(r, z_{s2} = 2)$ versus $g_{m+s2-}(r, z_{s2} = 3)$. Finally, some gathering effect of counterions near the polymer has also been observed and is shown in figure 10. Like for the salt anions, the peaks are located extremely close to the monomers and their heights drop with n_{s1}. They are higher for the $z_{s1} = 4$, $z_{s2} = 2$ type of valence mixture than for $z_{s1} = 4$, $z_{s2} = 3$.

4. Summary

In this paper, using a version of the cooperative motion algorithm, we have carried out Monte Carlo simulations of a single, strongly charged chain, counterions and a mixture of two multivalent salts of different valences and concentrations at the fixed reduced temperature. The calculations have shown that the addition of salts reduces the system energy, leading to a tremendous decrease in the polymer size and effective charge. The last effect is, in turn, due

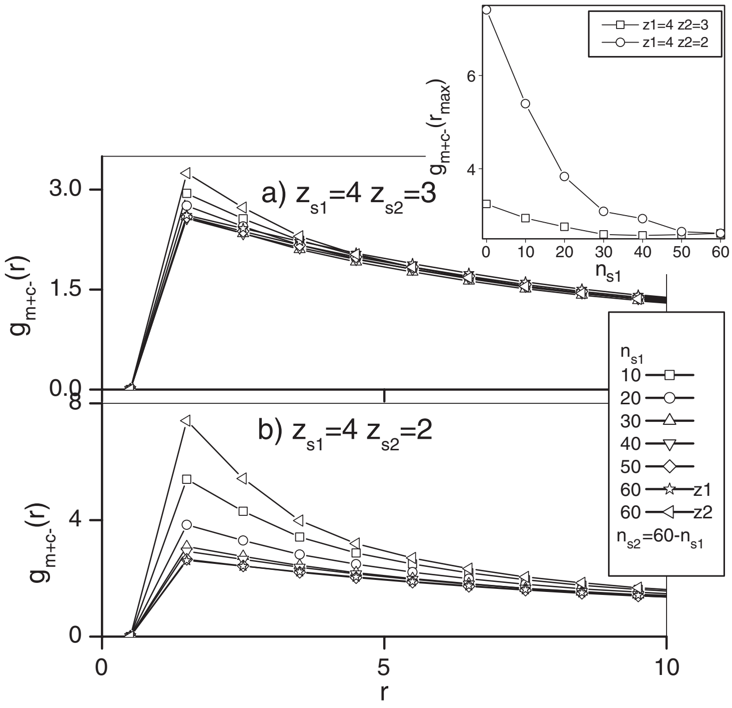

Figure 10. (a) The monomer–counterion PCF $g_{m+c-}(r)$ for $T^* = 1.0, n_{s1} = 10, 20, 30, 40, 50, 60$, $z_{s1} = 4$, $z_{s2} = 3$, (b) the same as in (a) except $z_{s2} = 2$. The inset shows the peak heights versus n_{s1} for $z_{s1} = 4$, $z_{s2} = 3, 2$.

to condensation of ions onto the polymer that, as indicated by the PCFs, is dominated by the multivalent salt ions with charges of sign opposite to that of the monomers.

Acknowledgments

This work was supported by Marie Curie European Reintegration Grant SIMPOL, MERG-CT-2004, Contract No 6348. The authors wish to acknowledge the Poznan Supercomputing and Networking Centre were the calculations were performed. J Kłos is very grateful to the late T Pakula for fruitful collaboration.

References

[1] Dünweg B, Stevens M and Kremer K 1995 *Monte Carlo and Molecular Dynamics Simulations in Polymer Science* ed K Binder (New York: Oxford University Press) p 125
[2] Olvera de la Cruz M, Belloni L, Delsanti M, Dalbiez J P, Spalla O and Drifford M 1995 *J. Chem. Phys.* **103** 5781
[3] Solis F J and Olvera de la Cruz M 2000 *J. Chem. Phys.* **112** 2030
[4] Solis F J and Olvera de la Cruz M 2001 *Eur. Phys. J.* E **4** 143
[5] González-Mozuelos P and Olvera de la Cruz M 2003 *J. Chem. Phys.* **118** 4684
[6] Schiessel H and Pincus P 1998 *Macromolecules* **31** 7953
[7] Manning G S 1969 *J. Chem. Phys.* **51** 924
[8] Manning G S 1969 *J. Chem. Phys.* **51** 934
[9] Manning G S 1969 *J. Chem. Phys.* **51** 3249

[10] Manning G S 1988 *J. Chem. Phys.* **89** 3773

[11] Stevens M J and Kremer K 1995 *J. Chem. Phys.* **103** 1669

[12] Takashima J, Takasu M and Hiwatari Y 1989 *Phys. Rev.* A **40** 2706

[13] Winkler R G, Gold M and Reineker P 1998 *Phys. Rev. Lett.* **80** 3731

[14] Brilliantov N V, Kuznetsov D V and Klein R 1998 *Phys. Rev. Lett.* **81** 1433

[15] Victor J M and Hansen J P 1987 *Europhys. Lett.* **3** 1161

[16] Donley J P 2002 *J. Chem. Phys.* **116** 5315

[17] Deserno M, Holm C and May S 2000 *Macromolecules* **33** 199

[18] Dobrynin A V and Rubinstein M 2001 *Macromolecules* **34** 1964

[19] Limbach H J and Holm C 2001 *J. Chem. Phys.* **114** 9674

[20] Stevens M J and Plimpton S 1998 *Eur. Phys. J.* B **2** 341

[21] Chang R and Yethiraj A 2003 *J. Chem. Phys.* **118** 6634

[22] Hofmann T, Winkler R G and Reineker P 2001 *J. Chem. Phys.* **114** 10181

[23] Muthukumar M 2004 *J. Chem. Phys.* **120** 9343

[24] Liu S and Muthukumar M 2002 *J. Chem. Phys.* **116** 9975

[25] Hofmann T, Winkler R G and Reineker P 2001 *J. Chem. Phys.* **114** 10181

[26] Hofmann T, Winkler R G and Reineker P 2003 *J. Chem. Phys.* **119** 2406

[27] Sarraguça J M G, Skepö M, Pais A A C C and Linse P 2003 *J. Chem. Phys.* **119** 12621

[28] Liu S, Ghosh K and Muthukumar M 2003 *J. Chem. Phys.* **119** 1813

[29] Grosberg A Yu, Nguyen T T and Shklovskii B I 2002 *Rev. Mod. Phys.* **74** 329

[30] Nguyen T T and Shklovskii B 2001 *J. Chem. Phys.* **114** 5905

[31] Takahashi A, Kato N and Nagasawa M 1970 *J. Phys. Chem.* **74** 944

[32] Reddy M and Marinsky J A 1970 *J. Phys. Chem.* **74** 3884

[33] Deserno M and Von Grunberg H 2002 *Phys. Rev.* E **66** 011401

[34] Kakehashi R, Yamazoe H and Maeda H 1998 *Colloid Polym. Sci.* **276** 28

[35] Liao Qi, Dobrynin A V and Rubinstein M 2003 *Macromolecules* **36** 3386

[36] Liao Qi, Dobrynin A V and Rubinstein M 2003 *Macromolecules* **36** 3399

[37] Adams D J and Dubey G S 1987 *J. Comput. Phys.* **72** 156

[38] Pakula T 1991 *J. Chem. Phys.* **95** 4685
Pakula T 2004 Simulations on the completely occupied lattice *Simulation Methods for Polymers* ed M J Kotelyanskii and D N Theodorou (New York: Dekker) chapter 5

[39] Meropolis N, Rosenbluth A W, Rosenbluth N N, Teller A H and Teller E 1953 *J. Chem. Phys.* **21** 1087

[40] Kłos J and Pakula T 2005 *J. Chem. Phys.* **122** 134908